Interpretable Machine Learning for Modelling and Explaining Car Drivers' Behaviour: An Exploratory Analysis on Heterogeneous Data

Mir Riyanul Islam*[a], Mobyen Uddin Ahmed[b] and Shahina Begum[c]

Artificial Intelligence and Intelligent Systems Research Group, School of Innovation Design and Engineering,
Mälardalen University, Universitetsplan 1, 722 20 Västerås, Sweden
**Corresponding Author*

Keywords: Artificial Intelligence, Driving Behaviour, Feature Attribution, Evaluation, Explainable Artificial Intelligence, Interpretability, Road Safety.

Abstract: Understanding individual car drivers' behavioural variations and heterogeneity is a significant aspect of developing car simulator technologies, which are widely used in transport safety. This also characterizes the heterogeneity in drivers' behaviour in terms of risk and hurry, using both real-time on-track and in-simulator driving performance features. Machine learning (ML) interpretability has become increasingly crucial for identifying accurate and relevant structural relationships between spatial events and factors that explain drivers' behaviour while being classified and the explanations for them are evaluated. However, the high predictive power of ML algorithms ignore the characteristics of non-stationary domain relationships in spatiotemporal data (e.g., dependence, heterogeneity), which can lead to incorrect interpretations and poor management decisions. This study addresses this critical issue of 'interpretability' in ML-based modelling of structural relationships between the events and corresponding features of the car drivers' behavioural variations. In this work, an exploratory experiment is described that contains simulator and real driving concurrently with a goal to enhance the simulator technologies. Here, initially, with heterogeneous data, several analytic techniques for simulator bias in drivers' behaviour have been explored. Afterwards, five different ML classifier models were developed to classify risk and hurry in drivers' behaviour in real and simulator driving. Furthermore, two different feature attribution-based explanation models were developed to explain the decision from the classifiers. According to the results and observation, among the classifiers, Gradient Boosted Decision Trees performed best with a classification accuracy of 98.62%. After quantitative evaluation, among the feature attribution methods, the explanation from Shapley Additive Explanations (SHAP) was found to be more accurate. The use of different metrics for evaluating explanation methods and their outcome lay the path toward further research in enhancing the feature attribution methods.

1 INTRODUCTION

Artificial Intelligence (AI) and Machine Learning (ML) models are the basis of intelligent systems and continuously gaining popularity across diverse domains. The prime reason behind the models' growing popularity is the outstanding and accurate computation of features and the prediction based on the features. Among the AI/ML facilitated domains, the transportation domain is notably using different models within the framework of driving simulators. Driving simulators are increasingly adopted in different countries for diverse objectives, e.g., driver training, road safety, etc. (Sætren et al., 2019).

In conjunction with the increased demands on explanations for the decisions of AI/ML models in other domains, the need for explanation is also rising for the automated actions in the simulators. However, different fields from other domains are already facilitated with the eXplainable AI (XAI) research, e.g., anomaly detection (Antwarg et al., 2021), predictive maintenance (Serradilla et al., 2021), image processing (Wu et al., 2020) etc. conversely, road safety related simulator development and enhancement have been less exploited in XAI research. Though there are very few studies are available in the literature that explained the riding patterns of motorbikes (Abadi and Boubezoul, 2021), explaining drivers' fatigue pre-

[a] https://orcid.org/0000-0003-0730-4405
[b] https://orcid.org/0000-0003-1953-6086
[c] https://orcid.org/0000-0002-1212-7637

Islam, M., Ahmed, M. and Begum, S.
Interpretable Machine Learning for Modelling and Explaining Car Drivers' Behaviour: An Exploratory Analysis on Heterogeneous Data.
DOI: 10.5220/0011801000003393
In *Proceedings of the 15th International Conference on Agents and Artificial Intelligence (ICAART 2023) - Volume 2*, pages 392-404
ISBN: 978-989-758-623-1; ISSN: 2184-433X

diction (Zhou et al., 2021), etc., research studies on drivers' behaviours are scarce in terms of XAI. In addition, the research on the evaluation of explanations for the predictions or decisions of an AI/ML model is also in nurturing state.

Realising the need for research to enhance the simulation technologies and the complementary requirement for the development of the explanation models this research study was conducted. The main objective of the work presented in this paper can be outlined as-

- Explore the variation of drivers' behaviour in the simulator and track driving to enhance the simulator technologies.
- Develop classifiers for drivers' behaviour in terms of risk and hurry while driving.
- Explain the decisions of drivers' behaviour classifiers and evaluate the explanations.

The remaining sections of this paper are organised as follows: Section 2 introduces the materials and methodologies used in this study. The results and corresponding discussions on the findings are presented in Section 3. Finally, Section 4 contains the concluding remarks and directions for future research works.

2 MATERIALS AND METHODS

This section contains a detailed description of the experimental protocol, data collection, feature extraction, development of classifiers and explanation generation at local and global scope.

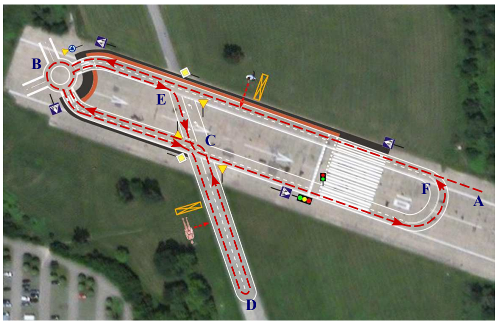

Figure 1: The experimental route for simulation and track tests. A detailed description is presented in Section 2.1.

2.1 Experimental Protocol

The experiment to collect data for this study was conducted under the framework of the European Union's Horizon 2020 project SIMUSAFE[1] (SIMUlation of behavioural aspects for SAFEr transport). Sixteen drivers were recruited for participating in the study. There were both male and female drivers. They were selected from two age groups 18-24 and 50+ years representing inexperienced and experienced drivers respectively. The participants were selected in such an order to have a homogeneous experimental group in terms of age, sex and driving experience. The participants were properly instructed about the experiments through information meetings. Informed consent and authorisation to use the acquired data in the research were obtained from each participant on paper. Throughout the experimental process, General Data Protection Regulation (GDPR) (Voigt and Von dem Bussche, 2017) was strictly followed.

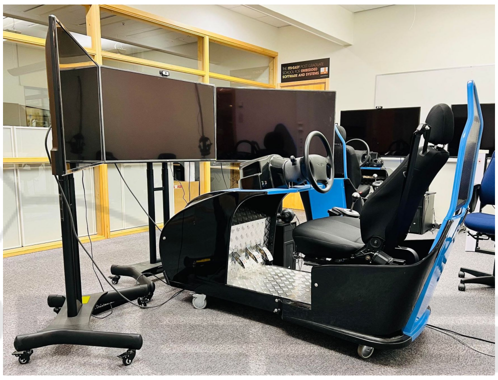

Figure 2: The car simulator developed with DriverSeat 650 ST was used for conducting the simulation tests.

The experimental protocol was outlined in accordance with the aim of the project SIMUSAFE; to improve driving simulator and traffic simulation technology to safely assess risk perception and decision-making of road users. To partially achieve the aim, the experiment was planned with the simulator and track driving tests. In both the simulation and track tests, participant drivers were required to drive along the identical route for seven laps with different variables. This design further facilitated the analysis of varying behaviour while driving on track and simulation. The route of the experiment is illustrated in Figure 1. For the track test, the route was prepared with proper road markings, signals etc. in an old airport in Kraków, Poland. In simulation tests, a modified variant of DriverSeat 650 ST (Figure 2) simulation cockpit was used. As annotated in Figure 1, each participant started the lap from point A, drove straight up to the roundabout at point B, took the third exit of the roundabout, drove up to point C to take a right turn, drove straight up to point D then took a U-turn and came back to point C for a left turn and then drove through points B (roundabout), E (right turn), C (left

[1] https://www.simusafe.eu/

Table 1: Associated scenarios for the laps of the experimental simulator and track driving with varying driving conditions.

Lap	Environmental Variables		Driver Variables				Scenario
	Events	**Traffic**	**Habituation**	**Hurry**	**Frustration**	**Surprise**	
1	Roundabout, Left Turn, Intersection with no Traffic Lights	No	Low	No	No	No	Drive along the route.
2			Low	No	No	No	
3			High	No	No	No	
4		Yes	High	No	No	No	
5		No	High	Yes	No	No	Drive along the route and finish as quickly as possible.
6		Yes	High	Yes	Yes	No	
7		No	High	No	No	Yes	Drive along the route.

turn) and finishes at point F after a left curve. For the simulation test, a similar route was designed virtually where the participants drove following the same protocol. In both tests, a participant drove through the route for seven laps with different scenarios containing varied environmental and driver variables as outlined in Table 1. The scenarios associated with the laps were designed with the consultation of psychologists and domain experts.

2.2 Data Collection

During the whole protocol, vehicular signals, physiological signals, psychological data and videos were recorded for each participant. In this study only the vehicular and physiological signals, specifically, EEG, have been exploited. All the data were properly anonymized to comply with the GDPR. The data collection methods and materials are briefly described in the following sections.

2.2.1 Vehicular Signal

The acquiring of the vehicular signals as numeric descriptive information was done using onboard instruments accessed via vehicle Controlled Area Network (CAN) and Inertial Measurement Unit (IMU). The signals contained information on the parameters like vehicle speed, acceleration, steering wheel angle, accelerator and brake pedal positions, Global Positioning System (GPS) coordinates, yaw, roll, pitch, etc. For track tests, the signals were directly acquired from the vehicle unit and for simulations, the measurements were recorded from the simulation framework. In both cases, the recording frequency was $15Hz$.

2.2.2 Biometric Signal

During both tests, i.e., simulation and track, the biometric signals in terms of EEG were recorded using the SAGA 32+ Systems[2] (TMSi, The Netherlands). Sixteen EEG channels ($Fp1$, Fpz, $Fp2$, $F7$, $F3$, Fz, $F4$, $F8$, $P7$, $P3$, Pz, $P4$, $P8$, $O1$, Oz, and $O2$), placed according to the 10–20 International System with a Brainwave EEG Head caps, were collected with a sampling frequency of $256Hz$, grounded to the Cz site. During the experiments, raw EEG data were recorded and afterwards digitally filtered using a band-pass filter ($2-70Hz$) in TMSi Saga Interface with FieldTrip (Oostenveld et al., 2011) integration. Finally, ARTE (Automated aRTifacts handling in EEG) (Barua et al., 2017) algorithm was used to remove the artefacts from the band-pass filtered signals. This step was necessary because the artefacts, e.g., eyes-blinks, could affect the frequency bands correlated to the target measurements. However, this method allows cleaning the EEG signal without losing data and without requiring additional sensors, e.g., electro-oculographic sensors.

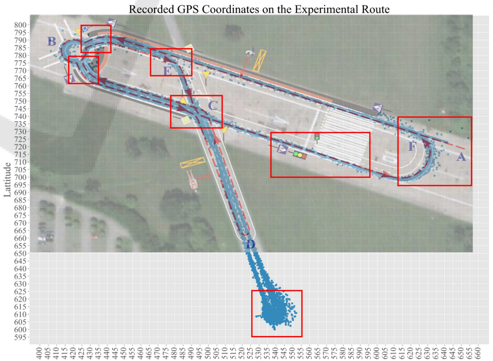

Figure 3: Event extraction using GPS coordinates. Red rectangles mark the significant areas of events, e.g., roundabout, left turn, signal with pedestrian crossing etc.

2.2.3 Event Extraction

The presented work within the framework of the SIMUSAFE project focused on risk perception, handling and hurry of drivers in urban manoeuvres that expose higher levels of risk. In risky situations, prime

[2] https://www.tmsi.com/products/saga-for-eeg/

events were short-listed by experts including roundabouts, left turns, extensive breaking/acceleration, etc. As per the experts' opinion, the events were defined based on the road infrastructure. To label the acquired data, all the GPS coordinates were plotted and overlaid on the experimental track to identify the specific GPS coordinates where an event could occur. Figure 3 illustrates the event extraction from GPS coordinates using overlaid scatter plot. Considering the GPS coordinates within the red rectangles in Figure 3 and consulting with domain experts and psychologists the data points were complemented with corresponding events. Figure 4 illustrates the recorded GPS coordinates of a single lap categorised on the basis of road infrastructure as events in different colours. The extracted events are further discussed in Section 3.1.

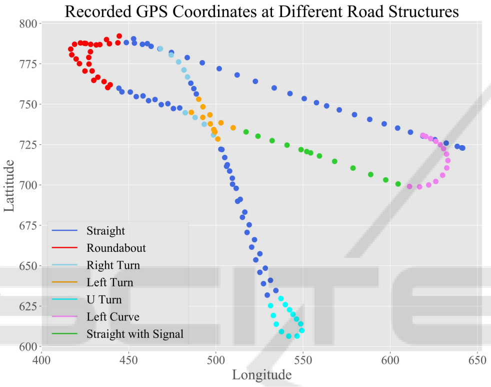

Figure 4: GPS coordinates of a single lap driving colour coded with respect to different road structures.

2.3 Dataset Preparation

The dataset for the presented work contains two separate sets of features and two different labels, i.e., risk and hurry. The features were extracted from the data collected from simulation and track tests. The process of feature extraction was performed in two folds after the events of interest were extracted through the utilisation of experts' annotation on the raw data, i.e. specific timestamps of the events' start and end. Based on the experts' annotation, for both vehicular and EEG signals, the raw data was chunked into epochs of 2 seconds using moving window with a shift of 0.125 second to preserve the condition of stationarity of the time-series data. Firstly, the vehicular features were extracted. In the second step, EEG features in the frequency domain were extracted and synchronised with the vehicular features on the basis of the timestamps of data recording. Finally, the dataset is prepared by combining the extracted features with the events and experts' annotated labels.

The vehicular feature sets were populated using the signals from vehicle CAN and IMU. The major features extracted from the vehicle CAN are speed, accelerator pedal position and steering wheel angle. The average and standard deviation of these measures were were calculated within the start and end time of the events annotated by the experts. These features were gathered in the feature list including the maximum value for speed only resulting in 7 features. From IMU, the parameters for angular and linear acceleration were considered and 9 features were calculated. All the features extracted from the vehicular signals are listed in Table 2.

Table 2: List of features extracted from vehicular signals.

Feature Name	Count	Source
Max. Speed	07	CAN
Avg. Speed		
Std. Dev. Speed		
Avg. Accelerator Pedal Pos.		
Std. Dev. Accelerator Pedal Pos.		
Avg. Steering Angle		
Std. Dev. Steering Angle		
Yaw	09	IMU
Yaw Rate		
Roll		
Roll Rate		
Pitch		
Pitch Rate		
Lateral Acceleration		
Longitudinal Acceleration		
Vertical Acceleration		

Avg.- Average, Max.- Maximum, Pos.- Position, Std. Dev.- Standard Deviation.

From the curated EEG signals, 14 frequency domain features were extracted from the power spectral density values. At first, the Individual Alpha Frequency (IAF) (Corcoran et al., 2018) values were estimated as the peak of the general alpha rhythm frequency ($8-12Hz$). Eventually, the average frequency of the theta band $[IAF-6, IAF-2]$, alpha band $[IAF-2, IAF+2]$ and beta band $[IAF+2, IAF+18]$, over all the aforementioned EEG channels were calculated. Next, the channels were partitioned on the basis of frontal and parietal locations on the scalp. For alpha and beta bands, frontal and parietal parts were again divided into two segments; upper and lower. For each of the segments, the average values of the frequency bands were considered as a feature, thus, obtaining a total of fourteen biometric features. Table 3 presents the list of the extracted biometric features that have been further deployed in classification tasks.

Table 3: List of biometric features considering different frequency bands of EEG signal.

Feature Name	Count	Source
Frontal Theta	14	EEG
Parietal Theta		
Frontal Alpha		
Lower Frontal Alpha		
Upper Frontal Alpha		
Parietal Alpha		
Lower Parietal Alpha		
Upper Parietal Alpha		
Frontal Beta		
Lower Frontal Beta		
Upper Frontal Beta		
Parietal Beta		
Lower Parietal Beta		
Upper Parietal Beta		

Summarising, a total of 30 features were extracted from the vehicular and biometric data recorded from the simulation and track tests. Among those, 16 features were extracted from the vehicle CAN & IMU sensors and 14 features were extracted from EEG signals. In addition to the libraries mentioned in respective sections, Python libraries NumPy and Pandas were also employed for data preparation.

After the feature extraction, the data points were clustered into various events as described in Section 2.2.3. For each event, the data point was labelled with associated risk and hurry based on the laps of the experimental protocol (Table 1) and psychologists' assessment. Each instance was labelled with 'yes' or 'no' for risk and hurry depending on their presence in the behaviour of the corresponding participant. The procedure produced 1771 data instances with varied numbers of instances for different labels of risk and hurry. Initially, the dataset was found to be largely imbalanced. To enhance the further analysis the instances with minority class for both risk and hurry were upsampled using SMOTE (Chawla et al., 2002). Table 4 presents the summary of the dataset.

2.4 Classifier and Explanation Models

This section briefly describes the models invoked in the presented work. Prior to the discussion on the models, the utilized dataset is theoretically formulated here. The data prepared as described in Section 2.3 is D comprising of feature set X and labels Y, i.e. $D = (X,Y)$. Each instance $x_i \in X$ where $i = 1,...,n$, contains features $f_j \in F$ where $j = 1,...,m$. The labels $y_i \in Y$ are associated with the corresponding instance $x_i \in X$ which varies on different classification tasks, i.e., risk and hurry. For all the tasks, D is split into D_{train} and D_{test} at a ratio of 80 : 20 respectively.

Table 4: Summary of the datasets from the simulator and track experiments for risk and hurry classification. The values represent the number of instances for corresponding labels of the classification tasks before applying SMOTE.

Classification	Label	Experiment		Total
		Simulation	Track	
Risk	Yes	330	215	545
	No	696	530	1226
Hurry	Yes	201	19	220
	No	825	726	1551
Total Instance		1026	745	1771

2.4.1 Classifier Models

The intended task is to classify risk and hurry separately which sets the context towards classification model $c(x_i)$. In all cases, $c(x_i)$ is trained using the instances of $X_{train} \subset X$ to predict the labels $\hat{y}_i$. The parameter tuning of $c(x_i)$ was performed by comparing the $\hat{y}_i$ and $y_i \in Y_{train} \subset Y$.

The selection of a candidate of $c(x_i)$ was done considering the performances of modelling car drivers' actions using different AI/ML models with a similar feature set from a previous work (Islam et al., 2020). Initially, four different classifiers have been tested to classify risk and hurry. The models are namely Logistic Regression (LR), Multilayer Perceptron (MLP), Random Forest (RF) and Support Vector Machine (SVM). In addition to these models, Gradient Boosted Decision Trees (GBDT) have been also tested for the described classification tasks. GBDT has been introduced in this study as an ensemble model which complements the use of different types of AI/ML models. The training parameters for all the models were tuned using grid search and 5-fold cross-validation. All the corresponding parameters for the selected models are presented in Table 5 that were tested in the grid search. The chosen parameters for the classifiers are also highlighted in the summary table. Python Scikit Learn (Pedregosa et al., 2011) library was invoked for training, validating and testing the classifier models.

2.4.2 Explanation Models

Literature indicates feature attribution methods are common choices for tabular data (Liu et al., 2021; Islam et al., 2022). A feature attribution method can be denoted as f that estimates the importance w of each

Table 5: Parameters used in tuning different AI/ML models for classifying risk and hurry in driving behaviour with 5-fold cross-validation. The parameters used for final training are highlighted in blue colour.

Classifier Models	Parameter Details
Gradient Boosted Decision Trees (GBDT)	Estimators: [100, 200, 300, 400, 500] Learning Rate: [$1e^{-3}$, $1e^{-2}$, $1e^{-1}$, 1] Max. Depth: [1, 3, 5, 7, 9] Loss : [*deviance*, *exponential*]
Logistic Regression (LR)	C: [$1e^{-4}$, $1e^{-3}$, $1e^{-2}$, $1e^{-1}$, 1, $1e^{1}$, $1e^{2}$, $1e^{3}$, $1e^{4}$] Penalty: [*l1*, *l2*] Solver: [*liblinear*]
Multilayer Perceptron (MLP)	Hidden layers: [$(32,16,8,4)$, $(32,16,4)$, $(16,8,4)$] Activation: [*identity*, *logistic*, *tanh*, *relu*] Alpha: [$1e^{-4}$, $1e^{-3}$, $1e^{-2}$] Solver: [*adam*, *lbfgs*, *sgd*]
Random Forest (RF)	Estimators: [10, 20, 30, 40, 50, 60, 70, 80, 90, 100] Criterion: [*gini*, *entropy*] Max. Features: [2^0, 2^1, 2^2, 2^3, 2^4, 2^5, 2^6, 2^7]
Support Vector Machine (SVM)	C: [1, $1e^{1}$, $1e^{2}$, $1e^{3}$] Gamma: [$1e^{-5}$, $1e^{-4}$, $1e^{-3}$, $1e^{-2}$, $1e^{-1}$, 1] Kernel: [*linear*, *poly*, *rbf*, *sigmoid*]

feature to the prediction. That is, for a given classifier model c and a data point x_i, $f(c,x_i) = \omega \in \mathbb{R}^m$. Here, each ω_j refers to the relative importance of feature j for the prediction $c(x_i)$. Among the feature attribution methods, Shapley Additive Explanations (SHAP) (Ribeiro et al., 2016) and Local Interpretable Model-Agnostic Explanation (LIME) (Lundberg and Lee, 2017) are exploited in this work as being popular choices in present research works (Islam et al., 2022). Both the explanation models were built for GBDT and D_test to generate local and global explanations. TreeExplainer was invoked for SHAP to complement the characteristics of GBDT and LIME was trained with default settings from the corresponding library.

2.5 Evaluation

The evaluation of the presented work has been performed in two folds: evaluating the performance of the classification models in classifying risk and hurry in drivers' behaviour and evaluating the feature attribution using SHAP & LIME to explain the classification. The metrics used for both evaluations are briefly described in the following subsections.

2.5.1 Metrics for Classification Model

Considering the binary classification for both risk and hurry, the confusion matrix (Figure 5) has been used as the base of the evaluation of classifier models, $c(x)$. In both the classification tasks, the presence of risk or hurry is considered as the positive label and absence is considered as the negative label. In the confusion matrix, True Positive (TP) and False Negative (FN) are the numbers of correct and wrong predictions respectively for the positive class, i.e., Yes (1). On the other hand, False Positive (FP) and True Negative (TN) are the numbers of wrong and correct predictions respectively for the negative class, i.e., No (0).

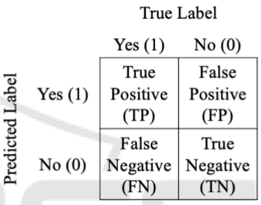

		True Label	
		Yes (1)	No (0)
Predicted Label	Yes (1)	True Positive (TP)	False Positive (FP)
	No (0)	False Negative (FN)	True Negative (TN)

Figure 5: Confusion Matrix for both Risk and Hurry Classification.

As described in Section 2.3 the dataset was prepared as a balanced dataset. Considering this, the metrics to evaluate the performance of $c(x)$ are selected to be Accuracy, Precision, Recall and F_1 score as prescribed (Sokolova and Lapalme, 2009).

2.5.2 Metrics for Explanation Model

The performances of the explanation models were measured using three different metrics; accuracy, Normalized Discounted Cumulative Gain (nDCG) score (Busa-Fekete et al., 2012) and Spearman's rank correlation coefficient (ρ) (Zar, 1972).

The accuracy scores for the explanation models were computed as the percentage of local prediction by the explanation model that matches the classifier model, i.e., $\frac{|c(x) \equiv f(x)|}{|X_{test}|}$. This metric would reflect how close the explanation models mimic the prediction of the classifier models.

To assess the feature attribution, the order of important features from the explanation models and GBDT were considered to calculate the nDCG score and ρ. Both measures are used to compare the order of retrieved documents in information retrieval. Specifically, nDCG score produces a quantitative measure to assess the relevance between two sets of ranks of some entities. Here, these score values were used to evaluate the feature ranking by the explanation models in contrast with the prediction model. For nDCG, the values were calculated separately for all the instances together and individually which are denoted as $nDCG_{all}$ and $nDCG_{ind}$ respectively in Table 9. Similarly, ρ produced a similar measure to evaluate the quality of two vectors of ranks which was used in parallel to support the nDCG score. Further details on the computation of these metrics can be found in the respective articles (Busa-Fekete et al., 2012; Zar, 1972). In this work, the values are computed using methods from SciPy library for Python.

3 RESULTS AND DISCUSSION

The outcome of the performed analysis, classification tasks and explanation generation have been presented and discussed in this section with tables and illustrations. The illustrations were prepared by adopting different methods of the Matplotlib library of Python.

3.1 Exploratory Analysis

Aligning with the focus of project SIMUSAFE, i.e. enhancing the simulation technologies to make the traffic environment safer, the exploratory analysis was conducted. The outcome of the analysis was further utilised to develop training simulators for road users with more intelligent agents which is out of the scope of the work presented in this paper. Though, the insights explored from the analysis were used to create intuition on the classification tasks and explanation.

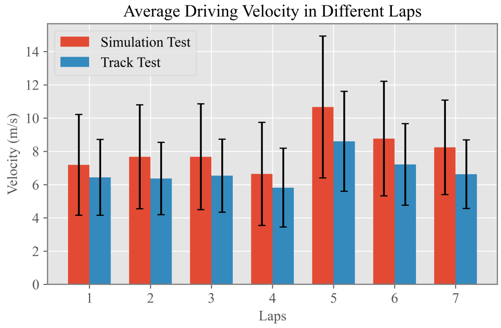

Figure 6: Average driving velocity in different laps. The two-sided Wilcoxon signed-rank test demonstrates a significant difference in the simulator and track driving with $t = 0.0, p = 0.0156$.

The first step of the analysis was performed to assess the variation of vehicular features between the simulation and track datasets over the laps that represent different road scenarios, interchangeably termed as events as described in Table 1. Mostly, mean values were compared and two-sided Wilcoxon signed-rank tests (Wilcoxon, 1992) were performed. In the significance test, the null hypothesis, H_0 was considered as "there is no difference between the observations of the two measurements". Subsequently the alternate hypothesis, H_1 was derived as "the observations of the two measurements are not equal" and the level of significance was set to 0.05. The first comparison was done on the driving velocity. Figure 6 illustrates the average driving velocity in different laps for simulation and track driving. The standard deviations are also associated with the respective error bars in the plot. For both tests, it was observed that average velocity increased in laps 5 - 7. This aligned with the experimental protocol. From the two-sided Wilcoxon signed-rank test, a statistically significant difference was observed between simulation and track driving ($t = 0.0, p = 0.0156$), thus the alternate hypothesis H_1 was accepted. The analysis on the accelerator pedal position (Figure 7) produced a similar trend across the laps for both the tests and the statistical test had identical outcomes.

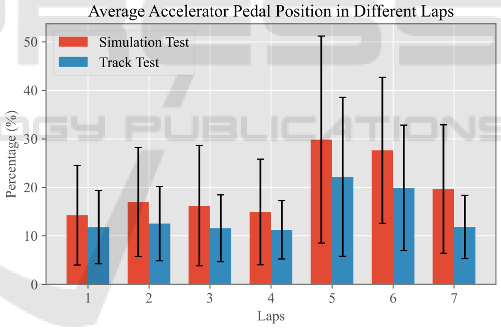

Figure 7: Average accelerator pedal position across all the laps and the two-sided Wilcoxon signed-rank test demonstrate a significant difference in the simulator and track driving with $t = 0.0, p = 0.0156$.

From both the analysis of driving velocity and accelerator pedal position, it was evident that drivers tend to drive at a higher velocity and press the accelerator pedal more in simulation tests than in track tests. This is plausibly the cause of simulator bias. In naive terms, drivers do not experience the motion of the vehicle, and perceive the environment properly, e.g, the vibration of the vehicle, the effect of road structures, etc. The differences in the driving behaviour have been properly addressed with corresponding experts and it is a work in progress to reduce the simulation biases in future studies. Moreover, while de-

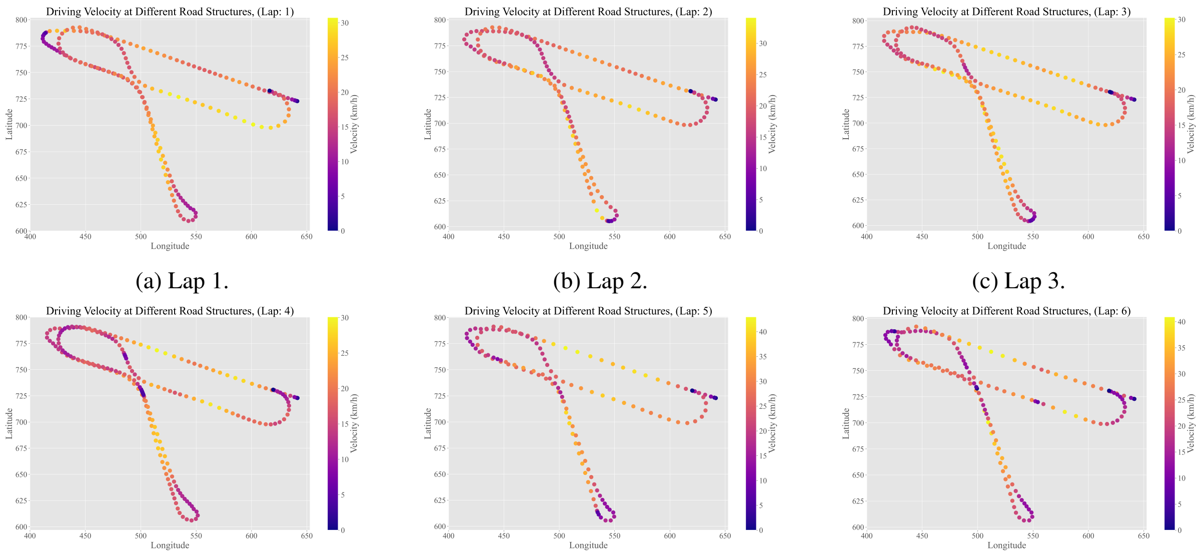

(a) Lap 1.

(b) Lap 2.

(c) Lap 3.

(d) Lap 4.

(e) Lap 5.

(f) Lap 6.

Figure 8: GPS coordinates with varying driving velocity for a random participant in laps 1 - 6.

ploying ML algorithms to classify drivers' behaviour, these characteristics from non-stationary spatiotemporal data might lead to incorrect interpretations. To correctly assess the effects or contribution of the heterogeneous features, two different methods of XAI were evaluated and presented in Section 3.3.

The driving velocity in each lap was also analysed based on different road structures using scatter plots and heatmaps as illustrated in Figure 8. In this analysis, the seventh lap was excluded because of the presence of surprise which reduced the data from driving the full lap. The pattern of driving velocity in laps 1 - 3 (Figure 8a - 8c) was found to be identical. The variation increased in laps 4 - 6 (Figure 8d - 8f) when several variables were added to the lap scenarios. The illustrated driving patterns were cross-checked with psychologists' assessments of the participants and their conclusive drivers' rules of behaviour. For example, on a left turn, the behaviour of drivers can be stated as - *'if the road is one carriageway, then you have to gradually move on the left and look for cars coming from the opposite direction before turning left'*. In all the sub-figures of Figure 8, it can be observed that, at the left turn near longitude 500 and latitude 750, the driver slowed down to examine oncoming vehicles and moved towards left before the turn as to road was single carriageway by design. Another major observation can be found in lap 6 at the lower middle of the circuit near longitude 550 and latitude 725 (Figure 8f). There was a signal with a pedestrian crossing and the driving velocity was close to zero which indicates that the stop signal was lit or a pedestrian was crossing and the driver responded to the signal. Thus, drivers' behaviours at different events in terms of road infrastructures were analysed and the observations were put forward to respective experts for enhancing the quality of the agents in future simulators.

3.2 Classification

The classification of drivers' behaviour was done in two folds; risk and hurry. It is arguable that hurried driving can induce risk. On the contrary, hurriedness is often observed among drivers who drive safely. Driving safely refers to specific behaviours as an example is stated in Section 3.1. Based on the drivers' rules of behaviour proposed by the experts, classifying risk and hurry are considered separate tasks. The performance of the trained models on the holdout datasets for risk and hurry classification are presented in Tables 6 and 7 respectively. In both tasks apparently, GBDT excelled over other models. However, for all the datasets in both tasks, simpler ones among the investigated models produced better performance. The use of precision and recall was justified by the nature of the classification tasks which mostly concentrate the measures on classifying the positive class. In this work, the positive class was set to be the presence of risk and hurry in drivers' behaviour which is more important than classifying their absence. One notable behaviour was observed for RF that it performed poorly when used on the simulation and track dataset separately but on the combined dataset it produced the result for risk classification. In the case of hurry classification, the behaviour was quite altered.

Table 6: Performance measures of risky behaviour classification with the AI/ML models trained on the holdout test set of different datasets. The best values for each metric and each dataset are highlighted in blue colour. (Positive Class - *Risk*, Negative Class - *No Risk*).

Metrics	**Simulation Dataset**					**Track Dataset**					**Combined Dataset**				
	GBDT	**LR**	**MLP**	**RF**	**SVM**	**GBDT**	**LR**	**MLP**	**RF**	**SVM**	**GBDT**	**LR**	**MLP**	**RF**	**SVM**
TP	105	82	86	23	100	106	88	103	56	105	229	186	226	233	228
FN	15	38	34	97	20	0	18	3	50	1	8	51	11	4	9
FP	16	26	42	0	14	3	24	5	0	4	30	62	45	26	23
TN	112	102	86	128	114	109	88	107	112	108	199	167	184	203	206
Precision	0.868	0.759	0.672	1.0	0.877	0.972	0.786	0.954	1.0	0.963	0.884	0.75	0.834	0.900	0.908
Recall	0.875	0.683	0.717	0.192	0.833	1.0	0.830	0.972	0.528	0.991	0.966	0.785	0.954	0.983	0.962
F_1 score	0.871	0.719	0.694	0.322	0.855	0.986	0.807	0.963	0.691	0.977	0.923	0.767	0.89	0.940	0.934
Accuracy	87.50	74.19	69.36	60.89	86.29	98.62	80.73	96.33	77.06	97.71	91.85	75.75	87.98	93.56	93.13

Table 7: Performance measures of hurry classification with the AI/ML models trained on the holdout test set of different datasets. The best values for each metric and each dataset are highlighted in blue colour. (Positive Class - *Hurry*, Negative Class - *No Hurry*).

Metrics	**Simulation Dataset**					**Track Dataset**					**Combined Dataset**				
	GBDT	**LR**	**MLP**	**RF**	**SVM**	**GBDT**	**LR**	**MLP**	**RF**	**SVM**	**GBDT**	**LR**	**MLP**	**RF**	**SVM**
TP	92	90	61	110	84	70	66	56	81	68	145	130	137	143	149
FN	18	20	49	0	26	11	15	25	0	13	25	40	33	27	21
FP	8	22	25	90	10	13	25	18	59	9	24	75	41	31	33
TN	91	77	74	9	89	65	53	60	19	69	174	123	157	167	165
Precision	0.920	0.804	0.709	0.550	0.894	0.843	0.725	0.757	0.579	0.883	0.858	0.634	0.770	0.822	0.819
Recall	0.836	0.818	0.555	1.0	0.764	0.864	0.815	0.691	1.0	0.840	0.853	0.765	0.806	0.841	0.876
F_1 score	0.876	0.811	0.622	0.710	0.824	0.854	0.767	0.723	0.733	0.861	0.855	0.693	0.787	0.831	0.847
Accuracy	87.56	79.90	64.59	56.94	82.78	84.91	74.84	72.96	62.89	86.16	86.69	68.75	79.89	84.23	85.33

Due to this fluctuation in the performance across different datasets and tasks, RF was not further utilized to develop the explanation models.

Table 8: Summary of model performances in terms of accuracy across different datasets and classification tasks.

Dataset		**Risk**	**Hurry**
Simulation	**Model**	GBDT	GBDT
	Accuracy (%)	87.50	87.56
Track	**Model**	GBDT	SVM
	Accuracy (%)	98.62	86.16
Combined	**Model**	RF	GBDT
	Accuracy (%)	93.56	86.69

Table 8 presents the best classifier for both risk and hurry classification across the three datasets. It is observed that overall GBDT performed better in every combination that lead to its use in the explanation generation. Moreover, to accumulate all the characteristics of the data in the explanation model only the combined dataset has been used further.

3.3 Explanation

Considering the prediction performance of GBDT across datasets and classification tasks, explanation models SHAP and LIME were built to explain individual predictions, i.e, local explanations. While explaining a single instance of prediction from c both models mimic the inference mechanism of c to predict the instance within their framework. The prediction performance of the explanation model was measured with local accuracy described in Section 2.5.2 and the values are presented in Table 9. It was observed that for both classification tasks, SHAP achieved higher accuracy than LIME. Moreover, LIME performed very poorly in local predictions for risk classification. However, both explanation models performed comparatively poorer in terms of hurry classification.

It is arguably presented in the literature that the feature importance value of a feature from a classifier is different in terms of weights from the contribution of the feature in an additive feature attribution model (Letzgus et al., 2022). However, normalizing the feature importance from GBDT and the contribu-

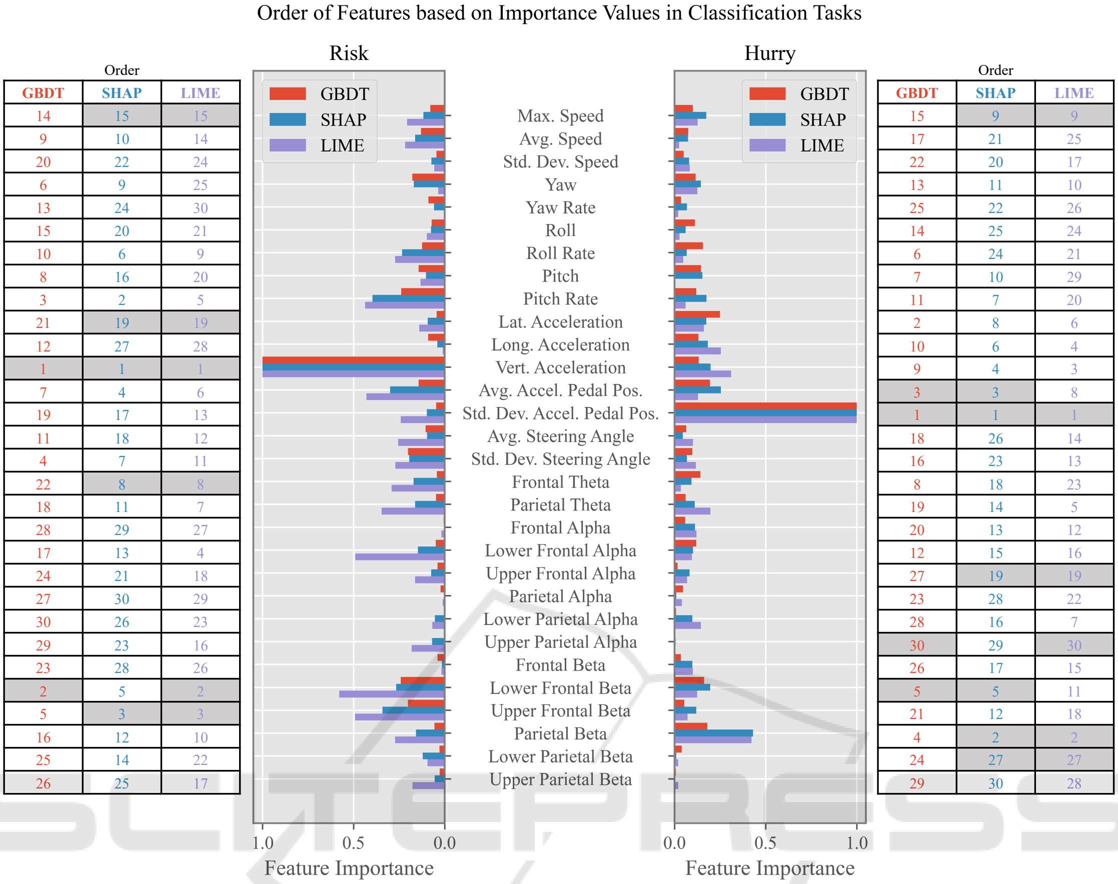

Risk GBDT	Risk SHAP	Risk LIME	Feature	Hurry GBDT	Hurry SHAP	Hurry LIME
14	15	15	Max. Speed	15	9	9
9	10	14	Avg. Speed	17	21	25
20	22	24	Std. Dev. Speed	22	20	17
6	9	25	Yaw	13	11	10
13	24	30	Yaw Rate	25	22	26
15	20	21	Roll	14	25	24
10	6	9	Roll Rate	6	24	21
8	16	20	Pitch	7	10	29
3	2	5	Pitch Rate	11	7	20
21	19	19	Lat. Acceleration	2	8	6
12	27	28	Long. Acceleration	10	6	4
1	1	1	Vert. Acceleration	9	4	3
7	4	6	Avg. Accel. Pedal Pos.	3	3	8
19	17	13	Std. Dev. Accel. Pedal Pos.	1	1	1
11	18	12	Avg. Steering Angle	18	26	14
4	7	11	Std. Dev. Steering Angle	16	23	13
22	8	8	Frontal Theta	8	18	23
18	11	7	Parietal Theta	19	14	5
28	29	27	Frontal Alpha	20	13	12
17	13	4	Lower Frontal Alpha	12	15	16
24	21	18	Upper Frontal Alpha	27	19	19
27	30	29	Parietal Alpha	23	28	22
30	26	23	Lower Parietal Alpha	28	16	7
29	23	16	Upper Parietal Alpha	30	29	30
23	28	26	Frontal Beta	26	17	15
2	5	2	Lower Frontal Beta	5	5	11
5	3	3	Upper Frontal Beta	21	12	18
16	12	10	Parietal Beta	4	2	2
25	14	22	Lower Parietal Beta	24	27	27
26	25	17	Upper Parietal Beta	29	30	28

Figure 9: Feature importance values are extracted from GBDT, SHAP & LIME, normalized and illustrated with horizontal bar charts for corresponding classification tasks. The order of the features based on the importance values is presented in tables on either side. Features with the same order across methods are highlighted in the order tables.

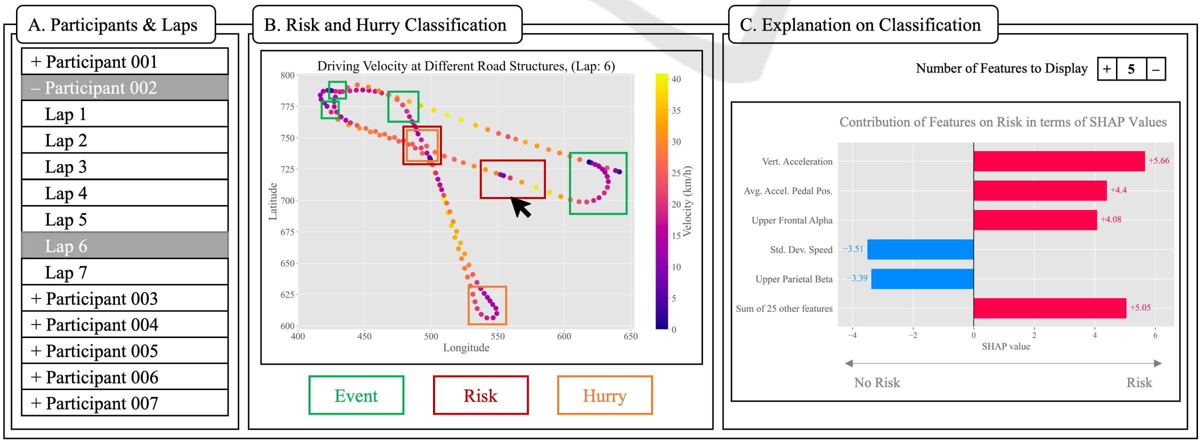
A. Participants & Laps
+ Participant 001
– Participant 002
Lap 1
Lap 2
Lap 3
Lap 4
Lap 5
Lap 6
Lap 7
+ Participant 003
+ Participant 004
+ Participant 005
+ Participant 006
+ Participant 007
B. Risk and Hurry Classification
Driving Velocity at Different Road Structures, (Lap: 6)
Latitude
Longitude
Velocity (km/h)
Event
Risk
Hurry
C. Explanation on Classification
Number of Features to Display + 5 –
Contribution of Features on Risk in terms of SHAP Values
Vert. Acceleration +5.66
Avg. Accel. Pedal Pos. +4.4
Upper Frontal Alpha +4.08
Std. Dev. Speed −3.51
Upper Parietal Beta −3.39
Sum of 25 other features +5.05
SHAP value
No Risk
Risk

Figure 10: Low fidelity prototype of proposed drivers' behaviour monitoring system for simulated driving.

tions from SHAP and LIME produced several similarities in the chosen order of features by the methods. For example, all three methods had the same feature as the most influential one in both tasks; vertical acceleration for risk and standard deviation of accelerator pedal position in hurry classification (Fig-

Table 9: Pairwise comparison of performance metrics for SHAP and LIME on combined X_{test} (holdout test set) for risk and hurry. For all the metrics, higher values are better and highlighted in blue colour. All the values for ρ are statistically significant since $P < 0.05$.

Metrics	**Risk**		**Hurry**	
	SHAP	**LIME**	**SHAP**	**LIME**
Accuracy	92.59%	52.98%	84.32%	70.06%
$nDCG_{all}$	0.9561	0.8758	0.9588	0.9183
$nDCG_{ind}$	0.8717	0.8589	0.8671	0.8524
ρ, P	0.7664, $7.91e^{-7}$	0.5310, $2.53e^{-3}$	0.7059, $1.31e^{-5}$	0.4772, $7.67e^{-3}$

ure 9). In risk classification, it is justified that vertical acceleration is the most contributing feature as it corresponds to the lifting of the front part of the vehicle due to sudden acceleration. In this scenario, the vehicle often gets out of control and the concerned events are - driving at the roundabout exits with pedestrian crossing, manoeuvring after a left turn, etc. In the other classification task for hurry, the standard deviation of the accelerator pedal position corresponds to a frequent pressing of the pedal with a varying intensity which is plausibly an indication to hurry. Here, the concerned events are similar to the events mentioned for risk.

Several similar ranks of the features based on their contributions from both SHAP and LIME motivated the comparison of *nDCG* scores that computes the similarity of retrieved information. In this work, the retrieved information is the order of features according to their importance values or contributions to prediction. The nDCG scores were computed for all the instances together and also computed for individual predictions and averaged. The rank of the features based on the normalized feature importance from the base model GBDT was used as the reference while calculating the *nDCG* score to assess how similar they are to the classifier model. Alike local accuracy, SHAP produced better results than LIME in terms of *nDCG* score. To investigate further, ρ was computed with a null hypothesis, 'the rank of the features in different methods are different'. However, with the test results, the hypothesis was rejected as all the measurements came out to be statistically significant as the P value was lower than 0.05. All the values of *nDCG* score and ρ are reported in Table 9. Another noteworthy aspect was observed from the metrics evaluating the explanation models that SHAP produced better results for risk classification but the performance of LIME was better for hurry classification. The performance of SHAP complements the performance summary of the classification models presented in Table 8 where risk classification had better performance than hurry classification. It is also plausible that, if the local accuracy of an explanation model is better, the rankings of the attributed features are also more relevant which is evident in the corresponding nDCG score and ρ values.

3.4 Proposed Interpretable System

Combining all the presented outcomes, a proposed system is designed for drivers' behaviour monitoring for simulated driving. Figure 10 illustrates a low-fidelity prototype of the proposed system. The prototype consists of three segments; A, B and C which also represent the flow of operation of the system. In segment A, a list of participants and their driven laps will be listed. Upon selecting a participant and specific lap, the GPS plot of the lap will be presented in segment B with a heatmap representing the driving velocity. Moreover, the events in terms of road infrastructure will be marked in green rectangles. The event rectangles will be coloured red and orange for the presence of risk and hurry respectively. For concurrent presence, there will be a double rectangle as shown in the illustration. In the next step, if an event with risk or hurry is clicked, segment C will present the contributing features to the specific classification and their contributions in terms of SHAP values. In the prototype, an explanation for the selected risky event is shown. For segment C, users can also set the number of contributing features to display in the top right corner. This system can be efficiently utilized to analyse drivers' behaviour to correct driving styles to ensure a safer road environment for all users. The information shown in segment C contains the features from both vehicle and EEG which are relevant to the risky and hurried behaviour of the drivers according to the literature. An expert from the corresponding domain can relate the change in feature values and their effect on the prediction and convey specific instructions to modify the drivers' behaviour to make their driving safer.

4 CONCLUSIONS AND FUTURE WORKS

The work presented in this paper can be summarised in three aspects: i) comparative analysis of car drivers' behaviour in the simulator and track driving for different traffic situations, ii) development of classifier models to detect risk or hurry in drivers' behaviour and iii) explaining the risk and hurry classification with feature attribution techniques with a proposed system for drivers' behaviour monitoring in simulated driving. The first outcome is found to be a novel analysis that includes experimentation with simulation and track driving. The second and third outcomes can be concurrently utilised in enhancing the simulator techniques to train road users for a safer traffic environment through the functional development of the proposed drivers' behaviour monitoring system.

The outcome of this study is encouraging in terms of explanation methods that require further research. The lack of prescribed evaluation metrics in the literature led to the use of different borrowed metrics from different concepts. However, the results showed promising possibilities to enhance and modify them for future works on the evaluation of explanation methods. Another possible research direction would be to improve the feature attribution methods to produce more insightful explanations.

ACKNOWLEDGEMENTS

This study was performed as a part of the project SIMUSAFE funded by the European Union's Horizon 2020 research and innovation programme under grant agreement N. 723386.

REFERENCES

Abadi, M. L. and Boubezoul, A. (2021). Deep neural networks for classification of riding patterns: with a focus on explainability. In *Proceedings of the 29th European Symposium on Artificial Neural Networks, Computational Intelligence and Machine Learning*.

Antwarg, L., Miller, R. M., Shapira, B., and Rokach, L. (2021). Explaining anomalies detected by autoencoders using shapley additive explanations. *Expert Systems with Applications*, 186:115736.

Barua, S., Ahmed, M. U., Ahlstrom, C., Begum, S., and Funk, P. (2017). Automated EEG Artifact Handling with Application in Driver Monitoring. *IEEE Journal of Biomedical and Health Informatics*, 22(5):1350.

Busa-Fekete, R., Szarvas, G., Elteto, T., and Kégl, B. (2012). An Apple-to-Apple Comparison of Learning-to-Rank Algorithms in terms of Normalized Discounted Cumulative Gain. In *ECAI 2012-20th European Conference on Artificial Intelligence: Preference Learning: Problems and Applications in AI Workshop*, volume 242. Ios Press.

Chawla, N. V., Bowyer, K. W., Hall, L. O., and Kegelmeyer, W. P. (2002). SMOTE: Synthetic Minority Over-Sampling Technique. *Journal of Artificial Intelligence Research*, 16:321–357.

Corcoran, A. W., Alday, P. M., Schlesewsky, M., and Bornkessel-Schlesewsky, I. (2018). Toward a Reliable, Automated Method of Individual Alpha Frequency Quantification. *Psychophysiology*, 55(7).

Islam, M. R., Ahmed, M. U., Barua, S., and Begum, S. (2022). A Systematic Review of Explainable Artificial Intelligence in terms of Different Application Domains and Tasks. *Applied Sciences*, 12(3):1353.

Islam, M. R., Barua, S., Ahmed, M. U., Begum, S., Aricò, P., Borghini, G., and Di Flumeri, G. (2020). A Novel Mutual Information based Feature Set for Drivers' Mental Workload Evaluation using Machine Learning. *Brain Sciences*, 10(8):551.

Letzgus, S., Wagner, P., Lederer, J., Samek, W., Müller, K.-R., and Montavon, G. (2022). Toward Explainable Artificial Intelligence for Regression Models: A Methodological Perspective. *IEEE Signal Processing Magazine*, 39(4):40–58.

Liu, Y., Khandagale, S., White, C., and Neiswanger, W. (2021). Synthetic benchmarks for scientific research in explainable machine learning. *arXiv preprint arXiv:2106.12543*.

Lundberg, S. M. and Lee, S.-I. (2017). A Unified Approach to Interpreting Model Predictions. *Advances in neural information processing systems*, 30.

Oostenveld, R., Fries, P., Maris, E., and Schoffelen, J.-M. (2011). FieldTrip: Open Source Software for Advanced Analysis of MEG, EEG, and Invasive Electrophysiological Data. *Computational Intelligence and Neuroscience*, 2011.

Pedregosa, F., Varoquaux, G., Gramfort, A., Michel, V., Thirion, B., Grisel, O., Blondel, M., Prettenhofer, P., Weiss, R., and Dubourg, V. (2011). Scikit-learn: Machine Learning in Python. *The Journal of Machine Learning Research*, 12:2825–2830.

Ribeiro, M. T., Singh, S., and Guestrin, C. (2016). "Why should I trust you?" Explaining the Predictions of any Classifier. In *Proceedings of the 22nd ACM SIGKDD international conference on knowledge discovery and data mining*, pages 1135–1144.

Sætren, G. B., Lindheim, C., Skogstad, M. R., Andreas Pedersen, P., Robertsen, R., Lødemel, S., and Haukeberg, P. J. (2019). Simulator versus Traditional Training: A Comparative Study of Night Driving Training. In *Proceedings of the Human Factors and Ergonomics Society Annual Meeting*, volume 63, pages 1669–1673. SAGE Publications Sage CA: Los Angeles, CA.

Serradilla, O., Zugasti, E., Ramirez de Okariz, J., Rodriguez, J., and Zurutuza, U. (2021). Adaptable and explainable predictive maintenance: semi-supervised deep learning for anomaly detection and diagnosis in press machine data. *Applied Sciences*, 11(16):7376.

Sokolova, M. and Lapalme, G. (2009). A Systematic Analysis of Performance Measures for Classification Tasks. *Information processing & management*, 45(4):427.

Voigt, P. and Von dem Bussche, A. (2017). The EU General Data Protection Regulation (GDPR). *A Practical Guide, 1st Ed., Cham: Springer International Publishing*, 10:3152676.

Wilcoxon, F. (1992). Individual Comparisons by Ranking Methods. In *Breakthroughs in statistics*, pages 196–202. Springer.

Wu, S.-L., Tung, H.-Y., and Hsu, Y.-L. (2020). Deep Learning for Automatic Quality Grading of Mangoes:

Methods and Insights. In *2020 19th IEEE International Conference on Machine Learning and Applications (ICMLA)*, Miami, FL, USA. IEEE.

Zar, J. H. (1972). Significance Testing of the Spearman Rank Correlation Coefficient. *Journal of the American Statistical Association*, 67(339):578–580.

Zhou, F., Alsaid, A., Blommer, M., Curry, R., Swaminathan, R., Kochhar, D., Talamonti, W., and Tijerina, L. (2021). Predicting Driver Fatigue in Automated Driving with Explainability. *arXiv preprint arXiv:2103.02162*.